

Correlations Among Defect Type, Photoconductivity and Photoreactivity of Doped TiO₂

Myong-Ho Kim[†], Soon-Il Lee, Tae-Kwon Song, Hyunwoong Park*, Wonyong Choi*, Han-Il Yoo** and Tae-Gone Park***

Department of Ceramics Engineering, ***School of Mechatronics, Changwon National University, 9 Sarim-Dong, Changwon, Gyungnam 641-773, Korea

*School of Environmental Science and Engineering, Pohang University of Science and Technology, Pohang 790-784, Korea

**School of Materials Science and Engineering, Seoul National University, Seoul 151-742, Korea

(Received 30 August 2001 • accepted 15 October 2001)

Abstract—The electrical conductivity (σ), photoconductivity and photocatalytic reactivity in doped crystalline TiO₂ were measured as a function of the oxygen partial pressure (P_{O₂}), temperature, doping type and UV irradiation. The P_{O₂} dependence of σ suggests that the predominant atomic defects in pure TiO₂ are oxygen vacancies (V_O[•]) and interstitial titanium ions (Ti_i^{••}), but the dominant defect is changed with P_{O₂} and temperature. The photoexcited electrons in reduced and/or n-type doped TiO₂ enhance both the photoconductivity and the photocatalytic reactivity by the reduction process. Therefore, these behaviors are strongly dependent on the electron concentration.

Key words: Defect Type, Photoconductivity, Photoreactivity, Charge Compensation, Doping Effect

INTRODUCTION

Nonstoichiometric titanium dioxide, which is classified as an oxygen-deficient n-type semiconductor, is one of the most extensively studied metal oxides, because it is one of the promising materials as a photocatalyst [Fujishima, and Honda, 1972; Kasuge et al., 1997; Jongh et al., 1997; Nakato et al., 1997; Chai et al., 2000], oxygen sensor [Tien et al., 1975; Baek et al., 1999], varistor, and oxide electrode [Zaban et al., 1997; Watanabe et al., 1976]. The photocatalytic mechanism is still controversial, although there are many articles reporting the correlation of photocatalytic activity with the physical properties of TiO₂ such as crystal structure, surface area, particle size, and so on [Ohtani et al., 1997]. The purpose of this research is to investigate the correlation between the photoconductivity and the photocatalytic reactivity in undoped and doped polycrystalline titanium dioxide.

In this work, the electrical conductivity, the photoconductivity, and the photocatalytic reactivity in crystalline rutile are measured and discussed as a function of the oxygen partial pressure, temperature, doping type and UV irradiation time.

EXPERIMENTAL

1. Sample Preparation

Reagent-grades of TiO₂, Nb₂O₅, Ta₂O₅, MnO, and Al₂O₃ were used as the starting materials. The powders were mixed with ZrO₂ balls, dried and pressed into a rectangular form at 2,000 kgf/cm². These pellets were sintered at 1,400 °C for 10 hrs in air. The sintered pellets of the rutile structure were ground to the thickness of 2 mm,

electroded with Pt paste and heat treated at 1,000 °C for 15 min.

2. Electrical Conductivity

After the sample was printed by Pt paste (Heraeus Co.) and annealed for 15 min at 1,000 °C, the sample for the electrical conductivity was attached to Pt wires (Φ0.2 mm) for the four point-probe method to eliminate nonohmic contact effects. Fig. 1 shows the apparatus for measuring electrical conductivity. The low oxygen partial pressure (P_{O₂}) was established by using CO/CO₂ or H₂/H₂O/Ar mixture as shown in Fig. 1. The established P_{O₂} was monitored with a Y₂O₃ stabilized zirconia (YSZ) oxygen sensor. The resistivity of the sample was measured as a function of temperature (700 °C-1,300 °C) and partial pressure of oxygen (10⁰-10⁻²³ atm). That was converted into electrical conductivity by the following equation

$$\sigma = \frac{L}{R \times A} (1/\Omega \cdot \text{cm}) \quad (1)$$

where R is resistance, A is the area of the sample, and L is probe spacing.

3. Photoconductivity

For the measurement of the photoconductivity by the six probe method, one face of the sample was illuminated by UV lamp (40 w, 254 nm) as shown in Fig. 2. The photoconductivity was calculated from Eq. (2)

$$\text{Photoconductivity} = (L/A)/(R_1 - R_2) \quad (2)$$

where R₁ is resistance after the UV irradiation and R₂ is dark resistance before the UV irradiation.

4. Photoreactivity

Iodide oxidation reaction was used in order to measure the photoreactivity of the photocatalysts [Kormann et al., 1988]. The valence band holes or hydroxyl radicals generated on illuminated TiO₂ surface oxidize iodide (I⁻) to I[•] radicals, which subsequently trans-

[†]To whom correspondence should be addressed.

E-mail: mhkim@sarim.changwon.ac.kr

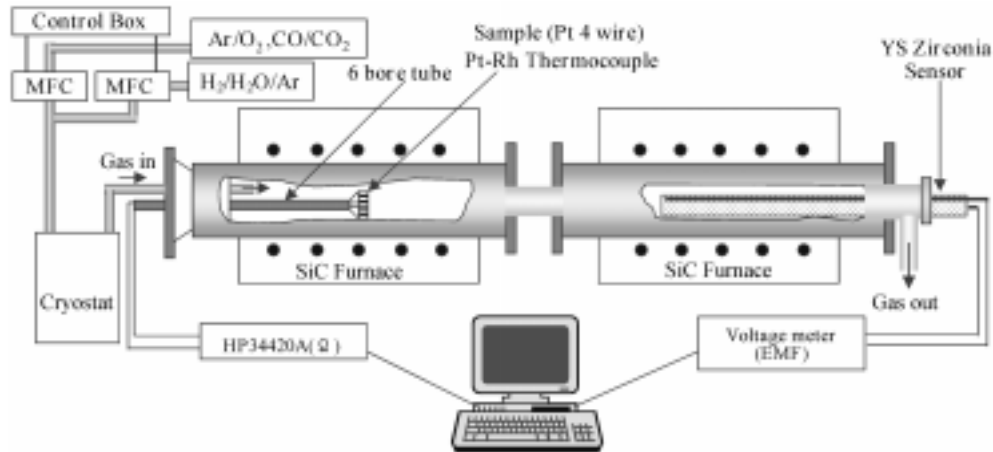


Fig. 1. Apparatus for measuring the electrical conductivity in oxygen partial pressure.

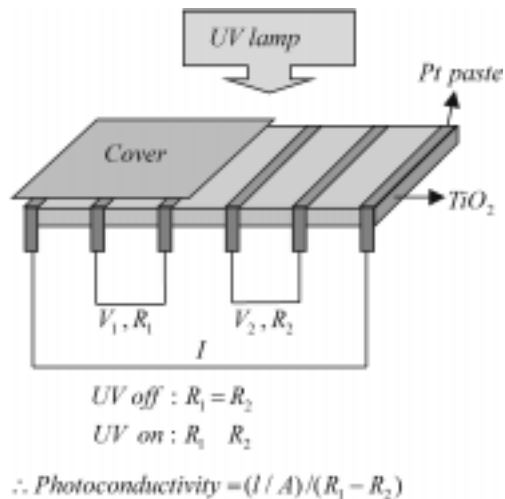


Fig. 2. Measurement of photoconductivity by the 6 point-probe method.

form to triiodide (I_3^-) through the following steps.



The triiodide production can be spectrophotometrically monitored by measuring the absorbance at 352 nm.

The photoreactivity test was performed as follows. Each photocatalyst prepared was coated on a slide glass and immersed in 30 ml of 0.01 M NaI solution. The solution pH was adjusted to 3. The photocatalytic oxidation of I^- occurs only in the acidic pH region and virtually no iodine or triiodide is formed at $\text{pH} > 7$ [Kormann et al., 1988]. The acidic condition is required for I^- to be electrostatically attracted onto the positively charged TiO_2 surface. Light from a 300 W Xe-arc lamp (Oriel) with $\lambda > 300$ nm was illuminated to the reactor. Then, the absorbance at 352 nm was measured after 1-hr illumination with a UV/Vis spectrophotometer (Shimadzu). The absorbance change corresponded to the photocatalytically generated I_3^- .

November, 2001

RESULTS AND DISCUSSION

1. Electrical Conductivity of Undoped TiO_2

Fig. 3 shows the oxygen partial pressure (P_{O_2}) dependence of the electrical conductivity (σ) in the temperature range between 700 °C and 1,300 °C. It is widely discussed in the literature that the dominant point defects in TiO_2 are oxygen vacancies and/or interstitial titanium ions [Balachandran and Eror, 1988; Tani and Baumard, 1980; Dirstine and Rosa, 1979].

As shown in Fig. 3, there is the change of the slope ($\sigma \log \delta \log P_{\text{O}_2}$) between $-1/4$ and $-1/5$ in the low P_{O_2} range. The electrical conductivity at temperatures above 1,100 °C is proportional to $P_{\text{O}_2}^{-1/5}$ in the intrinsic range (region I). The slope of $-1/5$ means that tetravalent charged interstitial titanium ions are dominant atomic defects above 1,100 °C by the reactions:



with the equilibrium constant at constant temperature.

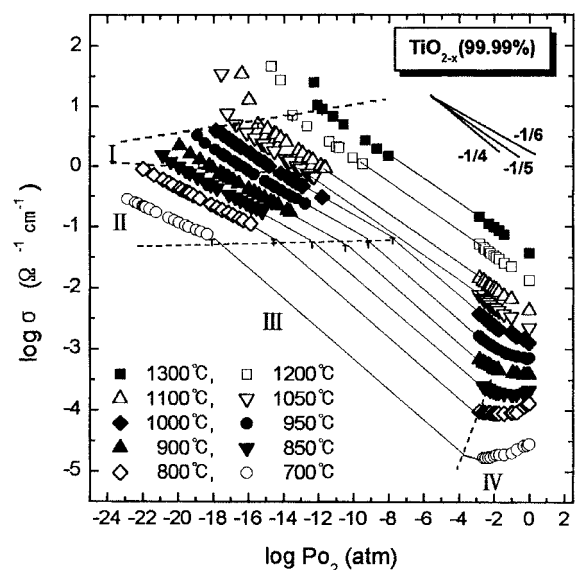


Fig. 3. Oxygen partial pressure dependence of electrical conductivity of undoped TiO_2 .

$$K_1 = [Ti_{i}^{+}]n^4Po_2 \quad (7)$$

The electroneutrality condition and the Po₂ dependence of an electron are given by

$$n = 4[Ti_{i}^{+}] = (4K_1)^{1/5}Po_2^{-1/5} \quad (8)$$

where n and Ti_{i}^{+} represent an electron and a tetravalent charged

titanium interstitial ion, respectively.

On the other hand, the σ values at temperatures below 1,100 °C have the Po₂ dependence of $-1/6$. The slope of $-1/6$ shows that doubly charged oxygen vacancies are predominant point defects in the region II. The formation of the doubly charged oxygen vacancies can be described as follows:



with the equilibrium constant at constant temperature

$$K_2 = [V_o^{2-}]n^2Po_2^{1/2} \quad (10)$$

The electroneutrality condition and the Po₂ dependence of an electron are given by

$$n = 2[V_o^{2-}] = (2K_2)^{-1/3}Po_2^{-1/6} \quad (11)$$

where V_o^{2-} is a doubly charged oxygen vacancy.

2. Electrical Conductivity of n-Type Doped TiO₂ (n-Type Doping Effect)

Figs. 4-5 show the electrical conductivity of TiO₂ doped with M₂O₅ (M=Ta or Nb) in dependence of the Po₂ and temperature. With the increasing M₂O₅ doping content, the slopes ($\delta \log \sigma / \delta \log Po_2$) change continuously between $-1/5$, 0, and $-1/4$. The slope change means that different kinds of point defect type and charge compensation in M₂O₅-doped TiO₂ occur according to the Po₂ and the doping con-

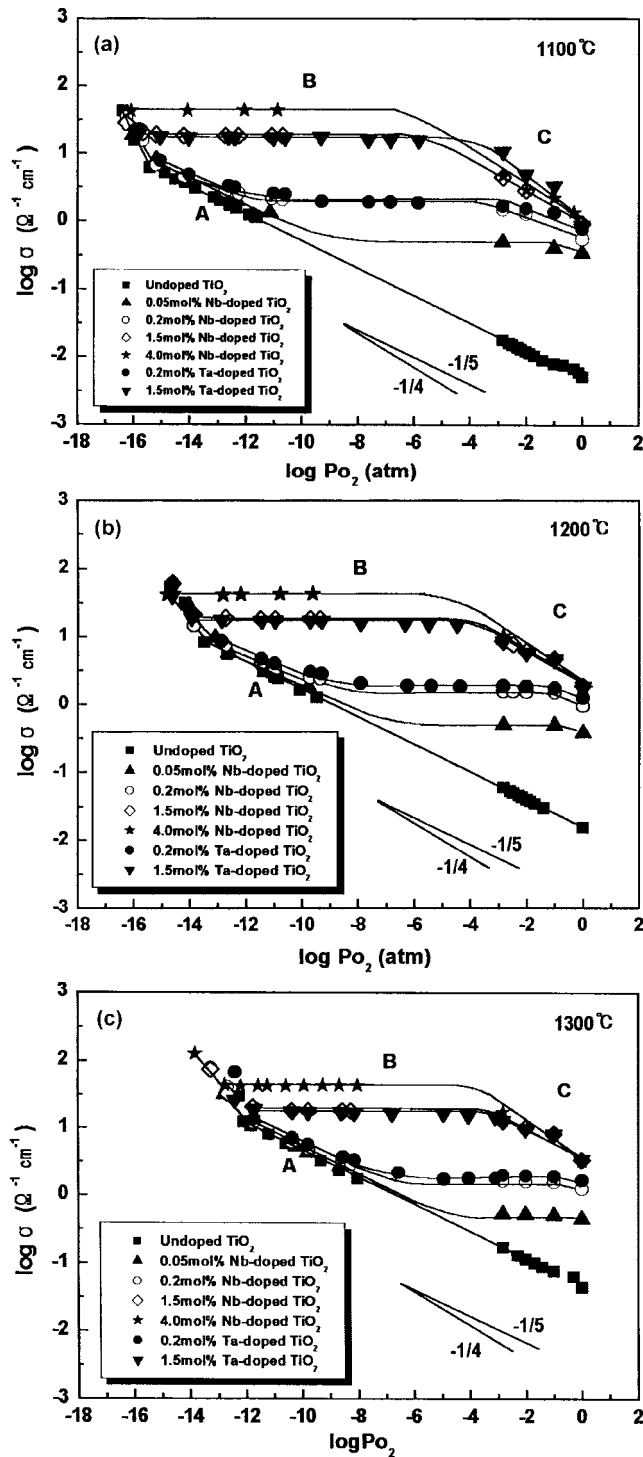


Fig. 4. Oxygen partial pressure dependence of electrical conductivity with the doping content of M₂O₅ (M=Ta or Nb) at (a) 1,100 °C, (b) 1,200 °C, and (c) 1,300 °C.

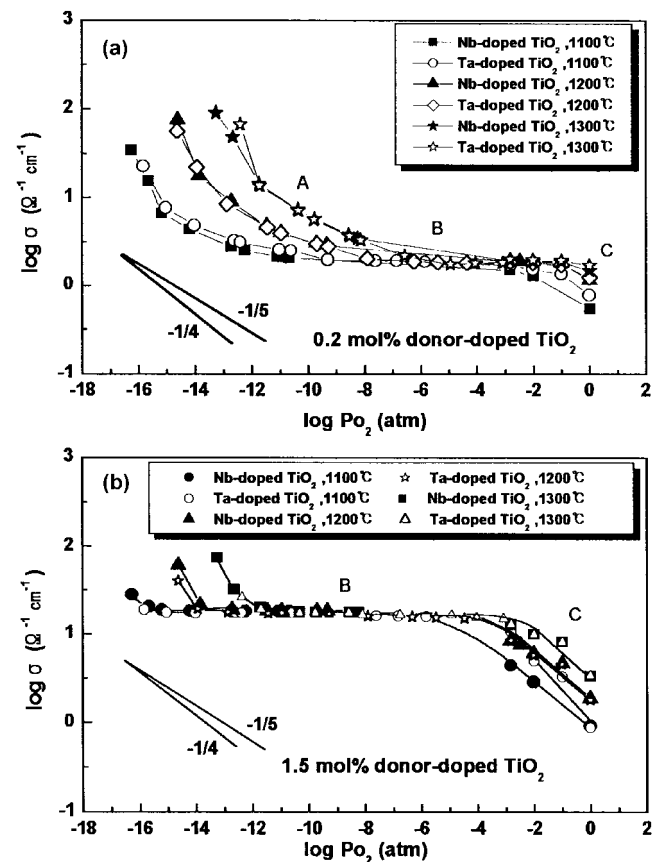
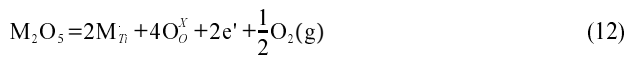


Fig. 5. Oxygen partial pressure dependence of electrical conductivity with temperature at (a) 0.2 mol% and (b) 1.5 mol% M₂O₅ (M=Ta or Nb) donor-doped TiO₂.

tent.

The electrical behavior in region B can be interpreted as follows:



The electroneutrality condition and the doping content dependence of the electrical conductivity are written by

$$\sigma \propto n = [M_{Ti}] \quad (13)$$

where M_{Ti} is a tantalum or niobium ion occupying a titanium lattice site.

The conductivity in region B is independent of temperature and P_{O_2} , but strongly dependent on the M_2O_5 doping content.

In region C where the P_{O_2} dependence of σ shows $-1/4$, the formation of the titanium vacancy is suggested as follows:



The electroneutrality condition in region C is given by

$$[M_{Ti}] = 4[V_{Ti}^{m}] \quad (15)$$

where V_{Ti}^{m} is a titanium vacancy.

According to the experimental results in region B and C, the mechanism of the charge compensation changes from electronic compensation (region B) to ionic compensation (region C) with the increasing P_{O_2} .

Details of the charge compensation and the defect reactions in region B and C were reported elsewhere [Lee et al., 1999; Chiang et al., 1997].

3. Electrical Conductivity of p-Type Doped TiO_2 (p-Type Doping Effect)

As shown in Fig. 6, the electrical conductivity of Al_2O_3 doped TiO_2 decreases slightly with the increasing Al_2O_3 doping content. The electrical behavior in Fig. 6 can be described by the defect reaction and the electroneutrality condition:



$$[Al_{Ti}^+] = 4[Ti_i^{m}] \quad (17)$$

where Al_{Ti}^+ represents an aluminum cation occupying a titanium lattice site.

The electron concentration from Eq. (16) is given by Eqs. (6) and (7) as follows:

$$n = [Al_{Ti}^+]^{-1/4} (4K_1)^{1/4} P_{O_2}^{-1/4} \quad (18)$$

In this case, the conduction electron is inversely proportional to the doping content of Al_2O_3 , and correspondingly the electrical conductivity of Al_2O_3 doped TiO_2 will be decreased [Lee, 2001].

4. Photoconductivity and Photocatalytic Reactivity in TiO_2

The photoconductivity values obtained in dependence on the doping type, the doping content, and the redox treatment are summarized in Table 1. The photoconductivity of both the reduced TiO_2 and n-type doped TiO_2 samples shows higher values than that of the oxidized TiO_2 and p-type doped TiO_2 . The measured value also increases continuously with the n-type doping content.

In the case of the acceptor doped TiO_2 , however, the resistivity differs by several orders of magnitude. Therefore, the photocon-

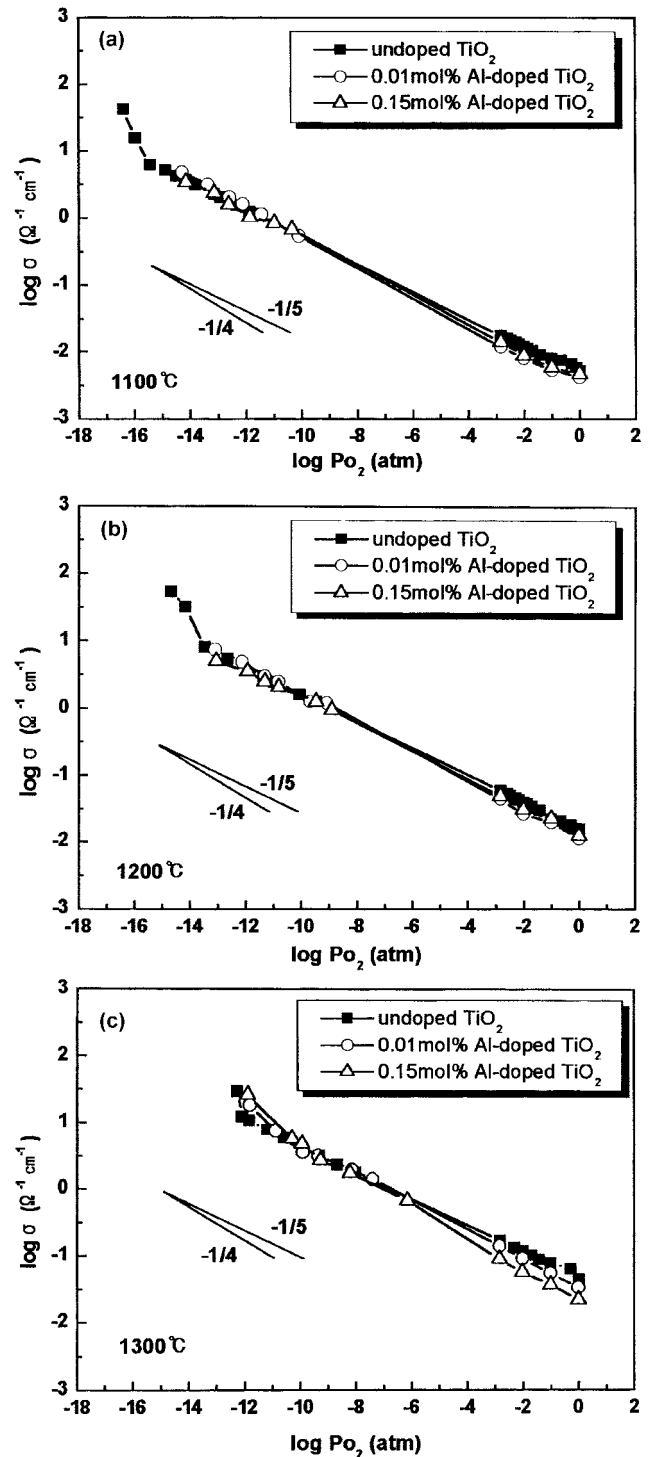


Fig. 6. Oxygen partial pressure dependence of electrical conductivity with the Al_2O_3 doping content at (a) 1,100 °C, (b) 1,200 °C, and (c) 1,300 °C.

ductivity can't be measured with the instrument (KIETHLY ELECTROMETER 6514) which can measure ohms up to giga ohm ranges ($10^9 \Omega$).

The electrical behavior in Al_2O_3 doped TiO_2 can be interpreted by Eqs. (16) and (17), as described in the p-type doping effect.

The photocatalytic reactivity of undoped and doped TiO_2 sam-

Table 1. Photoconductivity data of TiO₂ in dependence on the doping content, the doping type, and the redox treatment

Bulk sample	R ₁ (Ω) (UV off)	R ₂ (Ω) (UV on)	Photoconductivity $\sigma_{photo} = L / (R_1 - R_2) \times A$	Photo-efficiency $Y_{photo} = (R_1 - R_2) / R_1 \times 100$
Oxidized undoped-TiO ₂	nd	nd	.	.
Reduced undoped-TiO ₂	2.522k	2.221k	5.98×10^{-2}	11.93%
2.0 mol% MnO (p-type)	nd	nd		
0.2 mol% Al ₂ O ₃ (p-type)	nd	nd		
4.0 mol% Ta ₂ O ₅ (n-type)	544k	498k	3.91×10^{-4}	4.75%
1.5 mol% Ta ₂ O ₅ (n-type)	856k	817k	4.62×10^{-4}	4.56%

nd=not detected (>>1 GΩ).

Table 2. The photoreactivity of undoped and doped TiO₂. Absorbance at 352 nm was measured after 1 hr illumination

Bulk sample	A ₃₅₂
Undoped TiO ₂ (Oxidized at 0.21 atm)	0.0138
Undoped TiO ₂ (Reduced at 10 ⁻¹² atm)	0.0548
0.2 mol% Al ₂ O ₃ -doped TiO ₂	0.0168
2.0 mol% MnO-doped TiO ₂	0.0115
2.0 mol% Nb ₂ O ₅ -doped TiO ₂	0.1145

ples which was carried out by the photocatalytic oxidation of iodide is listed in Table 2. The n-type doped TiO₂ shows the highest value of the photocatalytic reactivity after the UV irradiation.

On the other hand, the reactivities of both undoped and p-type doped TiO₂ are similar.

From the experimental results, it is suggested that the photoexcited electron in a reduced and/or n-type doped TiO₂ can enhance the photoconductivity and also the photocatalytic reactivity by the reduction process, since the defect Ti_i^{••} and/or V_o for reduced samples and quasi-free electron by M_n for n-type doped samples play a significant role as charge transfer agent and an electron donor. It is expected that the photoconduction property by defect structure is similar to that of electrical conductivity. In other words, the photocatalytic reactivity by the oxidation process in a p-type doped and/or oxidized TiO₂ is negligible because the hole concentration is decreased by the charge compensation such as electron trapping of Al³⁺ site prohibited the Ti^{••}-O⁻ pair [Herrmann et al., 1984; Yamashita et al., 1998], although the oxidizing power of the hole is greater than the reducing power of the excited electron. It is observed that both the conductivity and the photocatalytic reactivity in this study are strongly dependent on the photoexcited electron concentration.

The measured data including the dominant point defects, photoconductivity, photoreactivity, and the doping type are summarized in Table 3.

CONCLUSIONS

In order to investigate the correlation among the dominant point defect, the photoconductivity and the photocatalytic reactivity, we measured the electrical conductivity, the photoconductivity and the photocatalytic reactivity as a function of the Po₂, temperature, doping type, and UV irradiation.

The results obtained in this study are summarized as follows:

1. The dominant atomic defect is changed with Po₂ and temperature, and the tetravalent charged interstitial titanium ions (Ti_i^{••}) and the doubly charged oxygen vacancies (V_o) are suggested in non-stoichiometric titanium dioxide.
2. The conductivity in n-type doped TiO₂ is strongly dependent on the doping content, and the mechanism of the charge compensation changes from electronic compensation to ionic compensation with the increasing Po₂.
3. The conductivity of p-type doped TiO₂ decreases with the increasing doping content.
4. The photoexcited electron in reduced and/or n-type doped TiO₂ enhances both the photoconductivity and the photocatalytic reactivity by the reduction process. Therefore, these behaviors are strongly dependent on the electron concentration in the defect structure of TiO₂.

ACKNOWLEDGEMENT

This work was supported by Korea Research Foundation Grant

Table 3. The defect types, electrical properties, and photo-properties of TiO₂

Sample	Region	Dominant defect	Electrical conductivity	Photo-conductivity	Photo-reactivity
Undoped TiO ₂	I	Ti _i ^{••}	$\sigma \propto n \propto \text{Po}_2^{-1/5}$		
	II	V _o	$\sigma \propto n \propto \text{Po}_2^{-1/6}$		
Reduced TiO ₂	I, II	Ti _i ^{••} , V _o	high	high	high
Oxidized TiO ₂			not detected	not detected	low
Doped TiO ₂					
Donor	II	e [•]	$\sigma \propto n = [M_n]$	high	high
Acceptor	III	V _n ^{•••}	$\sigma \propto n \propto \text{Po}_2^{-1/4}$		
	II	Ti _i ^{••}	$\sigma \propto n \propto \text{Po}_2^{-1/4}$ $\sigma \propto p \propto \text{Po}_2^{1/4}$	not detected	low

(KRF-99-042-E00109).

REFERENCES

- Baek, S. B., Lee, S. I. and Kim, M. H., "Microstructure and Electrical Properties of W-doped TiO₂," *Korean J. Mater. Res.*, **9**, 57 (1999).
- Balachandran, U. and Eror, N. G., "Electrical Conductivity in Nonstoichiometric Titanium Dioxide at Elevated Temperatures," *J. Mater. Sci.*, **23**, 2676 (1988).
- Chai, Y. S., Lee, J. C. and Kim, B. W., "Photocatalytic Disinfection of *E. coli* in a Suspended TiO₂/UV Reactor," *Korean J. Chem. Eng.*, **17**, 633 (2000).
- Chiang, Y. M., Birnie, D. and Kingery, W. D., "Physical Ceramics," John Wiley and Sons, Inc., 131 (1997).
- Dirstine, R. T. and Rosa, C. J., "Defect Structure and Related Thermodynamic Properties of Nonstoichiometric Rutile (TiO_{2-x}) and Nb₂O₅ Doped Rutile," *Z. Metallkunde, Bd.*, **70**, H. 5, 322 (1979).
- Fujishima, A. and Honda, K., "Electrochemical Photolysis of Water at a Semiconductor Electrode," *Nature*, **37**, 238 (1972).
- Herrmann, J. M., Disdier, J. and Pichat, P., "Effect of Chromium Doping on the Electrical and Catalytic Properties of Powder Titania under UV and Visible Illumination," *Chem. Phys. Letters*, **108**, 618 (1984).
- Jongh, P. E. and Vanmaekelbergh, D., "Investigation of the Electric Transport Properties of Nanocrystalline Particulate TiO₂ Electrodes by Intensity-modulated Photocurrent Spectroscopy," *J. Phys. Chem. B*, **101**, 2716 (1997).
- Kasuga, T., Hiramatsu, M., Hirano, M., Hoson, A. and Oyamada, K., "Preparation of TiO₂-Based Powders with Photocatalytic Activities," *J. Mater. Res.*, **12**, 607 (1997).
- Kim, M. H., Baek, S. B. and Paik, U. G., "Electrical Conductivity and Oxygen Diffusion in Nonstoichiometric TiO_{2-x}," *J. Korean Phys. Soc.*, **32**, S1127 (1998).
- Kormann, C., Bahnemann, D. W. and Hoffmann, M. R., "Preparation and Characterization of Quantum-Size Titanium Dioxide," *J. Phys. Chem.*, **92**, 5196 (1988).
- Lee, S. I., Baek, S. B. and Kim, M. H., "Electrical Properties and Defect Types of Nb-doped TiO₂," *The Kor. Ceram. Soc.*, **36**, 1135 (1999).
- Lee, S. I., "A Study on the Defect Types and Electrical Properties of TiO₂ Doped with Donor and Acceptor," M.S. Thesis, Changwon National University (2001).
- Nakato, Y., Akanuma, H., Magari, Y., Yae, J. I. and Mori, H., "Photoluminescence from a Bulk Defect near the Surface of n-TiO₂ (rutile) Electrode in Relation to an Intermediate of Photooxidation Reaction of Water," *J. Phys. Chem. B*, **101**, 4934 (1997).
- Tani, E. and Baumard, J. F., "Electrical Properties and Defect Structure of Rutile Slightly Doped with Cr and Ta," *J. Solid State Chem.*, **32**, 105 (1980).
- Tien, T. Y., Stadler, H. L., Gibbons, E. F. and Zacmanidis, P. J., "TiO₂ as an Air-to Fuel Ratio Sensor for Automobile Exhausts," *Ceramic Bulletin*, **54**, 280 (1975).
- Watanabe, T., Fujishima, A. and Honda, K., "Photoelectrochemical Reactions at SrTiO₃ Single Crystal Electrode," *B. Chem. Soc. Jap.*, **49**, 353 (1976).
- Yamashita, H., Kawasaki, S., Ichihashi, Y., Takeuchi, M., Harada, M., Anpo, M., Louis, C. and Che, M., "Characterization of Ti/Si Binary Oxides Prepared by the Sol-Gel Method and Their Photocatalytic Properties: the Hydrogenation and Hydrogenolysis of CH₃CCH with H₂O," *Korean J. Chem. Eng.*, **15**, 491 (1998).
- Zaban, A., Meier, A. and Gregg, A., "Electrical Potential Distribution and Short-range Screening in Nanoporous TiO₂ Electrodes," *J. Phys. Chem. B*, **101**, 7985 (1997).